ACS OMEGA

http://pubs.acs.org/journal/acsodf

Article

Synthesis and Evaluation of BSA-Loaded PLGA−Chitosan Composite Nanoparticles for the Protein-Based Drug Delivery System

Manish Gaur, Sarita Maurya, Mohd. Sohail Akhtar,* and Awadh Bihari Yadav*

Cite This: *ACS Omega* 2023, 8, 18751−18759

Read Online

ACCESS | Metrics & More | Article Recommendations

ABSTRACT: The purpose of this study was to synthesize composite nanoparticles (NPs) based on poly(D,L-lactic-*co*-glycolic acid) (PLGA) and chitosan (CS) and evaluate their suitability for the delivery of protein-based therapeutic molecules. Composite NPs possess a unique property which is not exhibited by any other polymer. Unlike other polymers, only the composite NPs lead to improved transfection efficiency and sustained release of protein. The composite NP were prepared by grafting CS on the surface of PLGA NPs through EDC-NHS coupling reaction. The size of bovine serum albumin (BSA)-loaded PLGA NPs and BSA-loaded PLGA−CS composite NPs was 288 ± 3 and 363 ± 4 nm, respectively. The zeta potential of PLGA NPs is −18 ± 0.23, and that of composite particles is 19 ± 0.40, thus confirming the successful addition of CS on the surface of PLGA NPs. Composite NPs were characterized using dynamic light scattering, scanning/transmission electron microscopy, Fourier transform infrared spectroscopy, X-ray diffraction, release profile, and gel electrophoresis. The encapsulation efficiency of PLGA NPs was 88%. These composite NPs were easily uptaken by the A549 cell line with no or minimal cytotoxicity. The present study emphasizes that the composite NPs are suitable for delivery of BSA into the cells with no cytotoxicity or very little cytotoxicity, while maintaining the integrity of the encapsulated BSA.

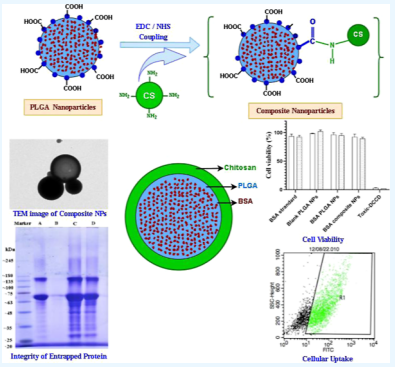

INTRODUCTION

The nanotechnology-based carrier is an emerging platform for the delivery of therapeutic molecules. The main focus of researchers remains to increase the efficacy of delivery without harmful effects. Different nanocarriers have been extensively investigated for delivering therapeutic molecules, which are biocompatible and biodegradable and do not impart any adverse effect.[1] The poly(D,L-lactic-*co*-glycolic acid) (PLGA) polymer-based delivery systems for being biocompatible and biodegradable have extensively been evaluated for the delivery of proteins and peptides. PLGA is approved by the United States Food and Drug Administration (US FDA) for therapeutic applications.[2] PLGA is a synthetic polyester made up of copolymers of poly-lactic acid and poly-glycolic acid. PLGA hydrolyzes in the presence of water into lactic acid and glycolic acid, which are hydrophilic, diffusible, and further eliminated into carbon dioxide and water by normal metabolic pathways.

Conversely, there are certain disadvantages such as a high negative charge that limits PLGA nanoparticle (NP)-associated therapeutic molecule delivery into the cell and drug burst release, which hampers sustained release.[3] The initial burst release is associated with many factors such as the ratio of composition of lactic acid and glycolic acid, particle size, porosity, and polymer molecular weight. Chitosan (CS) is a linear polysaccharide derived from chitin made up of repeating units of *N*-acetyl-D-glucosamine and D-glucosamine. It possesses a positive charge due to the presence of amine groups ($-NH_2$) and exhibits non-toxic, biodegradable, and biocompatible properties.[4] CS is electrostatically or covalently coated on the surface of negatively charged PLGA NPs, which improves the bioavailability and sustained release of therapeutic molecules. CS offers good transfection efficiency in comparison to PLGA. Hence, the composite NPs based on PLGA and CS offer a blend of properties of polymers for good transfection efficiency and with less negative charge, which facilitate easier uptake by the cells. The positive charge on the surface of composite NPs improves the stability and prolonged release of biomolecules.[5]

Several therapeutic biomolecules and drugs are loaded into nanocarriers such as protein, peptide, aptamer, antibodies, DNA, and RNA (miRNA and siRNA).[6] The diverse functional aspect of protein in general cannot be mimicked by a simple chemical entity. The proteins also do not interfere with the other biochemical reactions and do not produce any adverse effects or elicit any immune response due to having their

Received: February 4, 2023
Accepted: May 4, 2023
Published: May 17, 2023

natural entity and, hence, are considered as better delivery candidates.[7]

In the present study, bovine serum albumin (BSA) was used as a model protein to evaluate its delivery into the cell using a PLGA−CS-based composite NP system. BSA (66.5 kDa) is a stable protein and composed of charged amino acids; hence, its hydrophilic nature helps remain associated with the core part of PLGA NPs. Many researchers have used BSA as a model protein for the evaluation of different delivery systems. In polymeric NPs, protein encapsulation is critical and has immense potential in the development of a suitable vehicle for the delivery of protein.[8]

RESULTS

Characterization of Composite NPs. Composite NPs were characterized for their optimal activity. These particles were characterized by different parameters such as size, charge, polydispersity index (PDI), surface morphology, and so forth. The size of blank NPs and PLGA−CS composite NPs was analyzed by dynamic light scattering-based equipment, and it was found to be 282 ± 2 and 345 ± 2 nm, respectively. The size of NPs was increased with the loading of BSA to become 288 ± 3 nm and composite NPs 363 ± 4 nm, respectively Table 1. The sizes of blank and BSA-loaded NPs do not change significantly; however, the sizes of composite NPs increased significantly either as blank or BSA loaded. The PDI of NPs did not change significantly between blank or BSA-loaded NPs or composite NPs, and it was found in the range of uniform size distribution of NPs. The zeta potential of blank NPs and blank composite NPs was −14 ± 0.7 and 24 ± 1.2 mV, respectively. Change in zeta potential confirms the conjugation of CS on the surface of NPs. The zeta potential difference was also observed in BSA-loaded NPs and BSA-loaded composite NPs, and it was found to be −17 ± 0.2 and 19 ± 0.4 mV, respectively. The size, zeta potential, and PDI of NPs are shown in Table 1.

Table 1. Size, PDI, and Zeta Potential of Blank, BSA-loaded NPs, Blank Composite NPs, and BSA-loaded Composite NPs[a]

S. No.	NPs	Z-average (nm) (average ± SD)	PDI	Zeta potential (mV) (average ± SD)
1	blank NPs	283 ± 2	0.12	−14 ± 0.7
2	BSA loaded NPs	288 ± 3	0.14	−18 ± 0.2
3	blank composite NPs	345 ± 2	0.22	24 ± 1.2
4	BSA-loaded composite NPs	363 ± 4	0.18	19 ± 0.4

[a]The values are shown here as the means ± standard deviation (n = 3).

NP Morphology. The NP morphology and size of PLGA−CS NPs were characterized by scanning electron microscopy (SEM) and transmission electron microscopy (TEM) imaging (Figure 1). The surface morphology of PLGA NPs and PLGA−CS NPs was found to be spherical with a smooth surface and uniform size distribution in the SEM (Figure 1A,B). The TEM image of BSA-loaded PLGA NPs showed spherical morphology with smooth surfaces with a size range of approximately 200−450 nm (Figure 1C). NPs showed a spherical dense structure, while PLGA−CS NPs showed two distinct layers: the inner is a solid dense polymeric core of PLGA and the outer with a distinct layer evenly surrounded by CS.

Composite NP Characterization. The composite nature of NPs was characterized by different techniques. The composite nature of NPs was characterized by the zeta potential which increased significantly in comparison to PLGA NPs. We also characterized the composite nature of PLGA−CS NPs by TEM study. Figure 1D clearly suggests two distinct layers of polymers in the TEM image in which PLGA on the core is light, and CS is dark on the outer surface of NPs.

The composite NPs were also confirmed by Fourier-transform infrared (FTIR) spectra analysis. The FTIR spectra of all formulations and the polymers of PLGA and CS have been shown in Figure 2. The FTIR spectra of PLGA polymer were observed with characteristic peaks at 1,751 cm^{-1} (for C═O stretch of carbonyl group), 3,000−2,850 cm^{-1} (for C−H stretching vibration of −CH, CH_2, and CH_3 group), and 3,502 cm^{-1} (for −OH stretch). In CS, intense peaks were exhibited at 3,410 cm^{-1} (for N−H stretch overlapped with O−H stretch) and 1,628 cm^{-1} (for N−H bending of primary amine). Blank PLGA NPs, blank PLGA−CS NPs, BSA-loaded PLGA NPs, and BSA PLGA−CS NPs have represented similar peaks around 3,502 and 1,751 cm^{-1}, as presented on PLGA polymer. In comparison to PLGA NPs, PLGA−CS composite NPs have clearly shown stretching (around 3,500−3,000 cm^{-1}), indicating the successful conjugation of CS over PLGA NPs. The covalent conjugation of CS to the −COOH end group of PLGA by the formation of the amide bond was confirmed by the presence of a peak of amide I at 1,688 cm^{-1}. The FTIR spectra of BSA-loaded PLGA−CS NPs showed strong peaks at 3,503 and 1,763 cm^{-1}, which represented characteristic peaks of PLGA pure, and the 1,686 cm^{-1} peak of the amide bond confirmed the conjugation of CS to PLGA, which were seen in blank PLGA−CS NPs.

XRD Analysis. The results of the X-ray diffraction (XRD) analysis of BSA-loaded NPs and BSA-loaded PLGA−CS NPs are shown in Figure 3. The PLGA and CS polymers (Figure 3A,B) show a broad peak that represents their amorphous nature, while PLGA NPs (Figure 3C) show many sharp peaks and one intense peak at 20.50° that represents their crystalline nature with 65.96% crystallinity, indicating the successful synthesis of PLGA NPs. In comparison to PLGA NPs, blank PLGA−CS NPs (Figure 3D) show more intense peaks at 14.62, 18.78, and 23.41° with 87.33% crystallinity. The XRD pattern of BSA-loaded PLGA NPs shows more strong peaks (2θ values) at 20.38 and 23.41° with 83.56% crystallinity. The XRD pattern of BSA-loaded PLGA−CS NPs shows more intense peaks than the BSA PLGA NPs at 15.00, 19.21, 21.37, and 28.31° with 92.51% crystallinity. The PLGA−CS NPs show a higher crystalline structure in comparison to PLGA NPs.

Encapsulation Efficiency and Protein Loading. The encapsulation efficiency of BSA into NPs was estimated by an indirect method, and it was found to be 88%. The BSA loading into NPs was estimated by dissolving NPs, and it was estimated to be 24%.

Integrity Assessment. The integrity of encapsulated BSA into NPs was analyzed by running extracted BSA on SDS-PAGE and native PAGE gel electrophoresis. As shown in Figure 4A, SDS-PAGE, the band of BSA protein in wells C and D was intact and stable when we compared it with standard BSA protein in well A. The SDS-PAGE analysis of BSA encapsulated either with NPs or composite NPs shows that

https://doi.org/10.1021/acsomega.3c00738
ACS Omega 2023, 8, 18751−18759

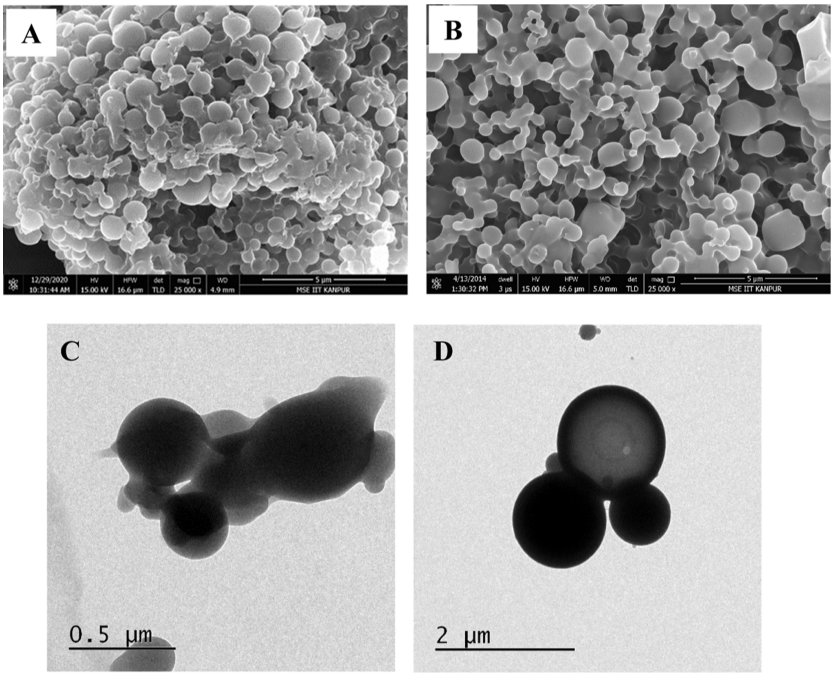

Figure 1. Micrographs of NPs and composite NPs. (A,B) NP morphology of PLGA NPs and PLGA−CS composite NPs by SEM; whereas, (C,D) are by TEM.

they are all stable (Figure 4A). The size of the BSA protein was also confirmed with a molecular weight marker at 66.5 kDa. In Figure 4B, the native gel was run with native BSA protein and extracted protein from three different formulations. As compared to the control, all the formulations show characteristics of a similar band movement, which shows that proteins retain their charge mass and structure without change during the process of encapsulation into NPs. In both studies, it was confirmed that the BSA loaded into NPs and composite NPs have not compromised their structural integrity.

Release Profile. The release profile of BSA from NPs and composite NPs was studied at a physiological pH of 7.4 over 96 h. In Figure 5, it was found that initially, NPs show burst release, where just in 4 h, it releases 50% of BSA and after that sustained and controlled release up to 96 h was found and release up to 96%. Composite NPs show improvement in burst release of BSA. Here, only about 32% release was observed in the initial 4 h followed by the sustained and controlled release of up to 78% in 96 h. CS-conjugated PLGA NPs show a moderate percentage drug release in comparison to PLGA NPs.

Uptake Study. The in vitro cellular uptake studies were performed to evaluate the efficiency of the uptake of PLGA NPs into A549 cell lines (adenocarcinoma human alveolar basal epithelial cells). Recently, the A549 cell line was used to analyze the internalization of dye-loaded polymeric NPs.[9] In current studies, fluorescein isothiocyanate (FITC) dye-loaded polymeric NPs were formulated and optimized for in vitro cellular uptake.[10] The flow cytometry analysis of FITC-loaded PLGA NPs and FITC-loaded PLGA−CS composite NPs were carried out to assess their intracellular uptake in A549 cells with incubation for about 4 h. With the observed gating and green color signal, the FITC uptake was observed to be enhanced in the viable cells (Figure 6). In Figure 6A, blank PLGA NPs show negligible uptake. In Figure 6B,C, FITC-loaded PLGA−CS composite NPs observed significantly increased intracellular uptake in 4 h in comparison to FITC PLGA NPs. The percentage of cellular uptake was found 40.34% in PLGA NPs and 56.12% in PLGA−CS NPs.

Cell Cytotoxicity Assay. Cell cytotoxicity assay was performed on A549 cells. A549 cells were exposed to NPs at different times. In Figure 7, cells exposed with an equal amount of BSA solution showed 92.45% cell viability, BSA-loaded NPs showed 95.02%, and BSA-loaded composite NPs showed 88.49% cell viability.

DISCUSSION

In this study, we synthesized composite NPs based on PLGA NP surface modification using EDS-NHS activation and CS grafting on the surface. Composite NPs offer unique properties that are not possessed by either CS or PLGA. These unique attributes include improved controlled release of payload, intensified percentage of crystallinity, and enhanced cellular uptake of the nanocarrier.

The primary aim of the study was to design a hybrid NP, which can efficiently deliver BSA inside the cells. Composite NPs were developed for efficient delivery of therapeutic proteins into the epithelial cells, which are present on the lung surface.[11] The stable PLGA NP formulation was successfully prepared in the same range of nanometer size confirmed by the PDI value. The encapsulation of BSA into NPs showed no significant difference in its size. The zeta potential of BSA-loaded NPs was found to have more negative charge, representing electrostatic charge interaction between polymers and payloads. BSA has an overall negative charge and, hence, the zeta potential increased more negatively.[12] The PLGA resomer has an acid end group (−COOH) at the terminal side of molecules, so it provides a negative charge to PLGA NPs. This −COOH group was used to graft CS on the surface of PLGA NPs. The change in zeta potential is a crucial indicator of the surface modification of the NPs. The surface charge represents the properties of the nanocarrier and the stability of

https://doi.org/10.1021/acsomega.3c00738
ACS Omega 2023, 8, 18751−18759

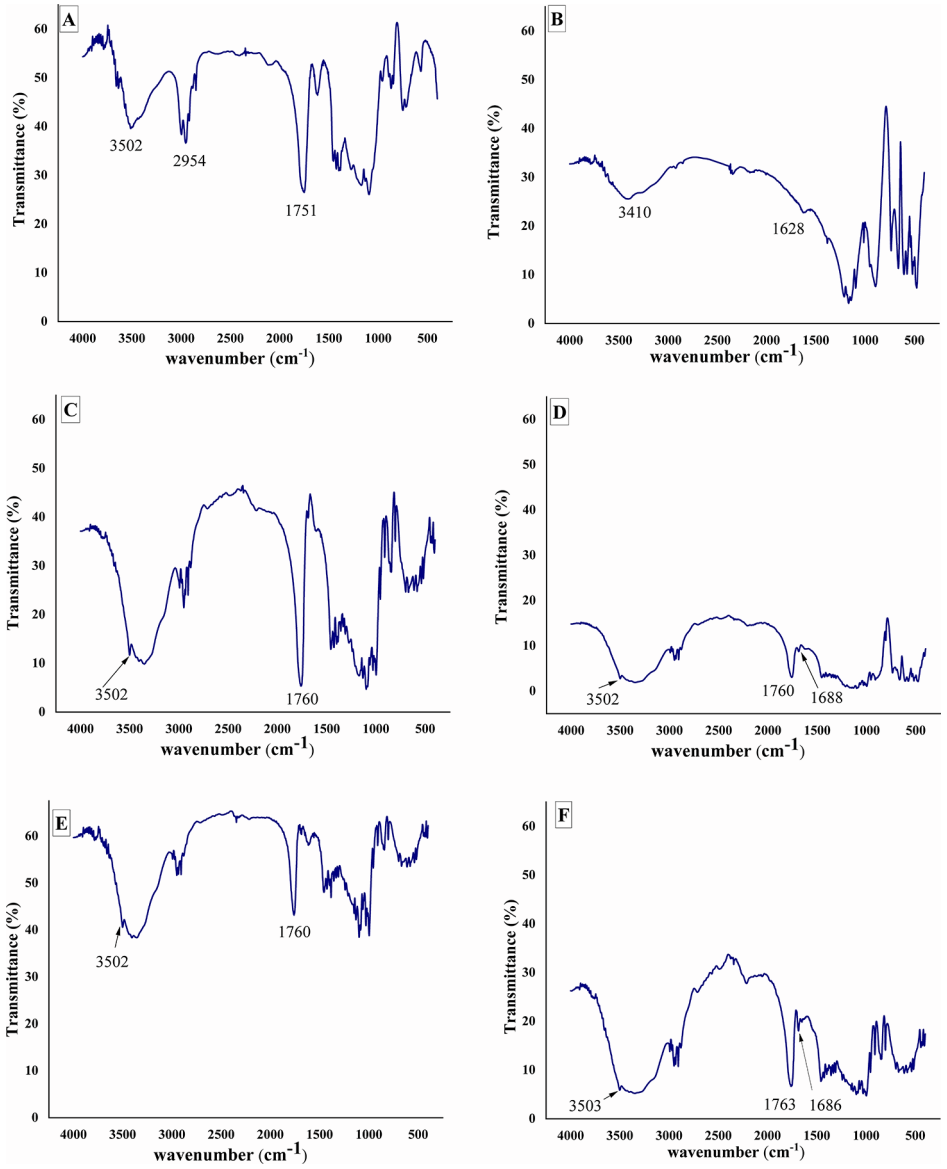

Figure 2. FTIR spectra of (A) PLGA powder, (B) CS powder, (C) blank NPs, (D) blank PLGA−CS NPs, (E) BSA-loaded PLGA NPs, and (F) BSA-loaded PLGA−CS NPs.

the drug delivery systems in the solution. A different approach can be used for surface modification, such as adsorption, incorporation, copolymerization, or covalent bonding, to modify PLGA NPs with CS.[13] In this study, we used covalent modification over other modifications and carried out an EDC-NHS coupling reaction. The carboxylic acid groups of PLGA NPs were activated with the EDC, which formed a stable intermediate with CS through amide bond formation. The successful surface modification of PLGA NPs was confirmed by the increase in the size of composite NPs as compared to PLGA NPs.[14] The zeta potential of composite NPs was changed from negative to positive charge that represented the successful grafting of CS on the surface of composite NPs. The zeta potential of BSA-loaded composite NPs had less positive charge in comparison to blank composite NPs because the BSA is negatively charged. The PDI represents the uniformity in the size distribution of NPs population, and its range varies between 0.0 and 1, where 0 represents the perfect uniform distribution of particle size and 1 represents high polydispersity with multiple particle size populations. For a polymeric NP, PDI values of 0.2 and below are reported most considerably in exercise.[15,16] The PDI values were 0.12, 0.14, 0.22, and 0.18, representing a relatively narrow particle size distribution. These data indicated that the PDI value of our particles lies in the uniform size range.

The surface morphology of the composite NPs was confirmed by SEM and observed as smooth, spherical in shape, and homogenous (Figure 1A,B). In TEM imaging, the composite nature of NPs was confirmed by two distinct layers within the particles (Figure 1D). The TEM imaging of composite NP clearly showed demarcations as two distinct internal and external layers, the core as PLGA, the outer layer as CS, and the center whitish part as the central blank part of PLGA NPs.[17,18]

The FTIR studies also confirm that the chemical conjugation of CS to PLGA NPs and BSA efficiently loaded into the NPs. In FTIR spectra (Figure 2), polymers were shown their characteristic peaks of stretching and bending, which confirms the presence of both polymers in the NPs.[14] In PLGA NP spectra (Figure 2C), peak intensities were

https://doi.org/10.1021/acsomega.3c00738
ACS Omega 2023, 8, 18751−18759

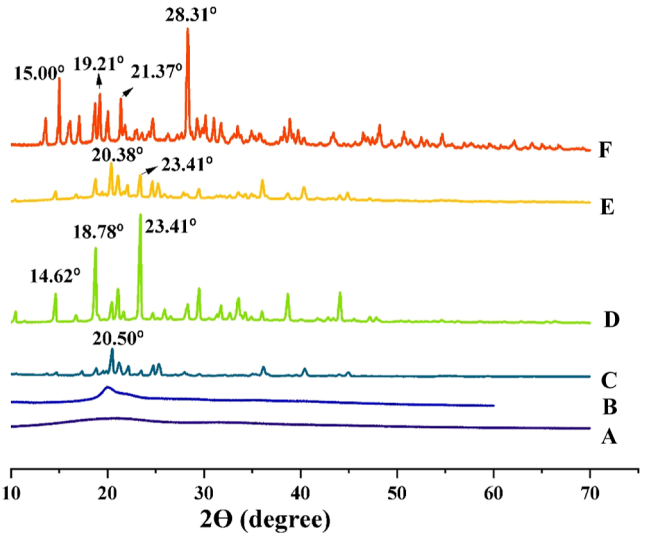

Figure 3. XRD analysis of (A) CS powder, (B) PLGA powder, (C) blank PLGA NPs, (D) blank PLGA−CS NPs, (E) BSA-loaded PLGA NPs, and (F) BSA-loaded PLGA−CS NPs, respectively.

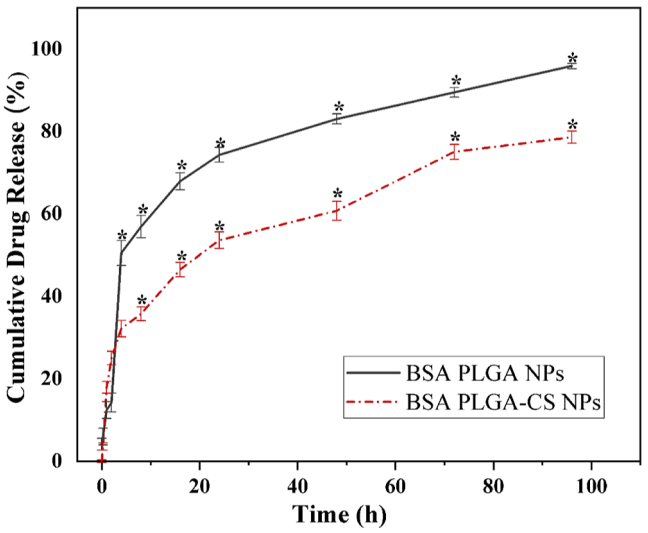

Figure 5. Percentage of BSA release from NPs (black) and PLGA−CS NPs (red) over 0−96 h at pH 7.4. Values are expressed as mean ± SD, * denoting significance at $p < 0.05$ value.

magnified, which represented the successful preparation of NPs. The peaks of C═O and O−H stretching have been increased due to the presence of these functional groups on the surface of NPs. In BSA-loaded NP and PLGA−CS composite NP spectra (Figure 2E,F), the main peaks of the amide I and amide II of BSA at 1670.1 and 1540.3 cm^{-1} were prominently masked by polymer bands. This confirmed the successful encapsulation of BSA into the PLGA matrix.[19] In spectra (Figure 2D,F), a new peak was observed at 1,688 and 1,686 cm^{-1}, which indicated the amide I bond (−CONH−) formed by the chemical conjugation of CS onto PLGA NPs through coupling reaction.[20] Peak broadening (Figure 2D,F) was observed, which shows the coating of CS over PLGA NPs. Due to the lack of no additional peaks, the FTIR analysis suggests the absence of interactions either between polymers or between protein and polymer.

The XRD pattern of PLGA and CS was not showing any distinct peaks (Figure 3), which indicated their amorphous nature.[21,22] The observed, distinct peaks of PLGA NPs (Figure 3C) represent their crystalline nature and successful fabrication.[23] After BSA encapsulation, the crystallinity of NPs increased, which indicates that BSA enhanced the crystallinity of the nanocarrier. It was also found that conjugation of CS to the NPs increased the crystallinity of the NPs via crosslinking reaction; however, non-conjugated PLGA NPs improved crystalline structure and arrangement of polymers as an entity.[24] The pattern of the XRD peaks of BSA-loaded composite NPs retained the characteristic peaks with reduced relative peak intensities with a slight shift in comparison to the BSA-loaded NPs, thus indicating the successful conjugation of CS onto the surface of PLGA NPs.[25,26]

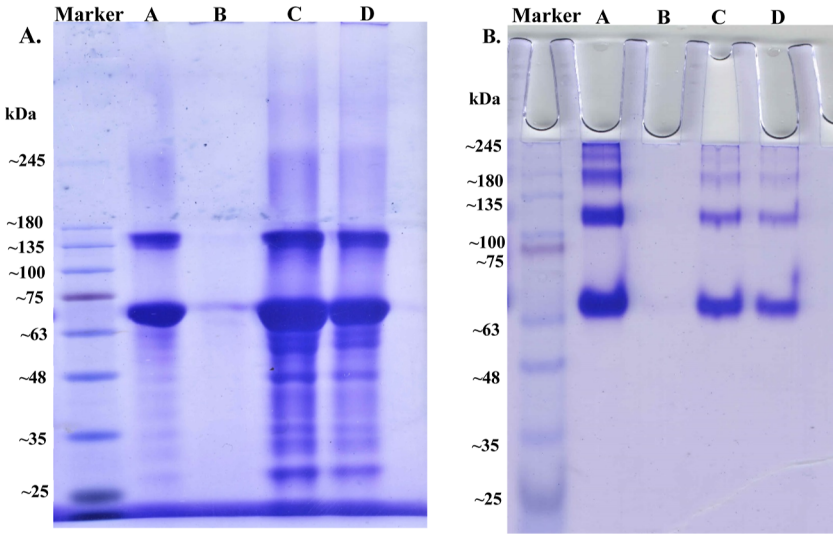

Figure 4. Integrity of encapsulated BSA into NPs and composite NPs was analyzed by (A) SDS-PAGE and (B) native gel electrophoresis. The different samples were loaded on the gel in different wells A: native BSA protein, B: blank NPs, C: BSA loaded NPs, and D: BSA loaded PLGA−CS composite NPs, respectively.

https://doi.org/10.1021/acsomega.3c00738
ACS Omega 2023, 8, 18751−18759

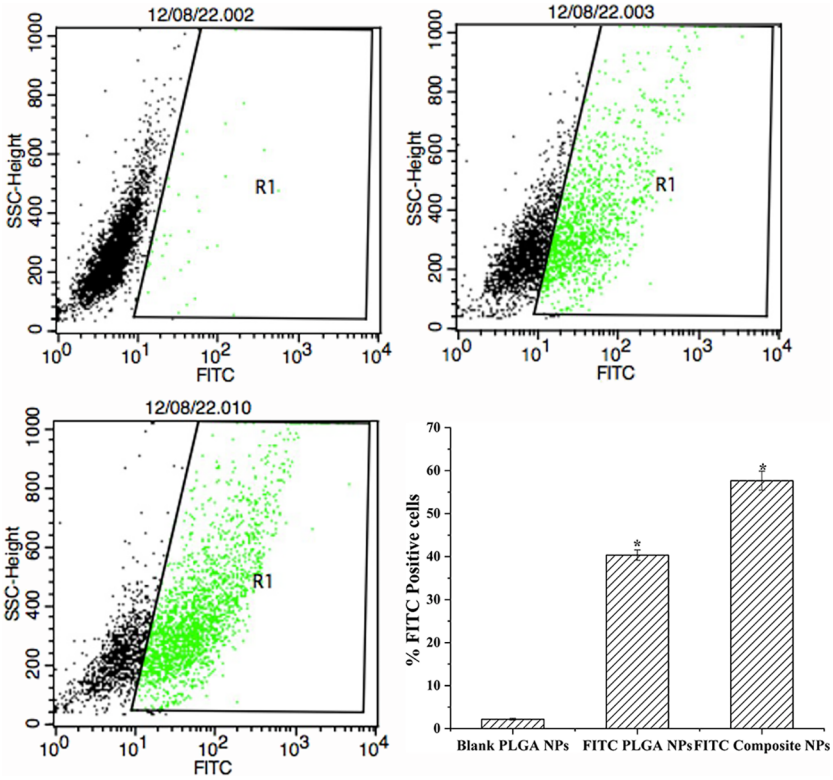

Figure 6. Cellular uptake of (A) blank PLGA NPs, (B) FITC-loaded PLGA NPs, (C) FITC-loaded PLGA−CS NPs by A549 cells, and (D) percentage of FITC-positive cells after exposure with a different formulation. * denotes significance at $p < 0.05$.

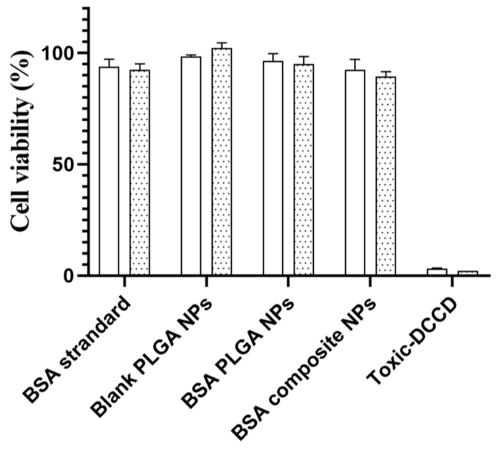

Figure 7. Cell cytotoxicity induced by composite NPs after exposure for (A) 24 h (hallow bar) and (B) 48 h (dotted bar) in the A549 cell line.

The SDS PAGE and native PAGE analysis were used to access whether the structural integrity of BSA might be compromised during NPs synthesis. Jin et al. prepared BSA-loaded NPs with different amounts of protein using the ultrasonication method. In this study, they found that the integrity of BSA was not compromised.[27,28] In SDS-PAGE gel electrophoresis, no degradation of BSA bands was observed in comparison to the loaded NPs. Furthermore, in native PAGE gel electrophoresis also, no degradation was observed (Figure 4). Results obtained in the gel electrophoresis study confirmed that the integrity of encapsulated BSA is retained during NP synthesis, which is very crucial to preserve the activity of protein during the encapsulation process; otherwise, it will hamper the efficacy of the therapeutic molecules.

The release of BSA from NPs is crucial for the development of successful therapy. It is essential for the therapeutic molecules to be released for a long time in a controlled manner. There are many factors that affect the release kinetics of PLGA NPs, some of them being the molecular weight and ratio of monomer lactic acid and glycolic acid can control drug release from the NPs. A high molecular weight of 50−150 kDa and a 50:50 ratio of monomer are suitable for the development of sustained drug-release formulations.[29] In a different study, it was reported that the end group of PLGA affects the degradation rate and increased water uptake.[30] PLGA NPs initially showed the burst release followed by the sustained release in PBS buffer, whereas in the case of PLGA−CS NPs, the burst phase was shorter, followed by prolonged release kinetics, and, hence, it acted better (Figure 5). CS grafting impaired net positive charge over negative charged PLGA NPs that improved mucoadhesive properties and sustained release of drugs as reported by a different research group in their study.[31] In our cellular uptake study, it was confirmed that the composite NPs were easily uptaken by the A549 cell line and that might be due to the improved interaction between cell and composite NPs in comparison to NPs (Figure 6). Hence, it may be assumed that the higher cellular uptake for protein-loaded composite NPs can be achieved by using BSA-loaded PLGA−CS NPs, where these particles also show improved sustained release of BSA. Here, it is observed that the cellular uptake of PLGA NPs was enhanced when their particle size was controlled below the sub-micron range.[32]

The compatibility of composite NPs was studied using resazurin assay. We quantified the number of live cells after exposure to different formulations and compared it with an

https://doi.org/10.1021/acsomega.3c00738
ACS Omega 2023, 8, 18751−18759

equivalent amount of BSA, BSA loaded into NPs, and BSA-loaded composite NPs exposed to the A549 cells. In all the cases, no significant cytotoxicity was observed. We also exposed cells to different amounts of NPs and found that cytotoxicity is dose-dependent, where more than 92% of cells were healthy after exposure to the highest amount of composite NPs (Figure 7). In this study, we found that our PLGA−CS composite NPs are also biocompatible and observed no toxicity after exposure to the cells.[33]

CONCLUSIONS

Our results showed that the protein-loaded PLGA NPs can be used for composite NPs synthesis by EDC NHS reaction without compromising the integrity of encapsulated protein into NPs. These composite NPs are efficiently taken by cells and show no significant level of cytotoxicity in the in vitro study on A549 cells. Composite NPs improved crystallinity and reduced burst release in comparison to BSA-loaded PLGA NPs. Hence, the study concludes that in comparison to PLGA NPs, the composite NPs can efficiently deliver the BSA into cells with better transfection efficiency. The CS PLGA composite NPs deliver the therapeutic protein into cells more effectively and show better promise for protein delivery systems for various purposes.

MATERIALS AND METHODS

Chemicals. Acid-terminated PLGA Resomer (lactide/glycolide copolymer, ratio M/M %:50/50, MW 24,000−38,000) and CS (from shrimp shells ≥75% degree of deacetylation) were purchased from Sigma Aldrich, USA. Dichloromethane (DCM) was purchased from Merck Life Science, India. Polyvinyl alcohol (PVA) and Resazurin dye were purchased from Merck, USA. EDC (*N*-(3-dimethylaminopropyl)-*N*′-ethylcarbodiimide hydrochloride), NHS (*N*-hydroxysuccinimide), and FITC (fluorescein-5-isothiocyanate) were purchased from Sigma-Aldrich, USA. Acetic acid glacial was purchased from Thermo Fisher Scientific, India. BSA was purchased from HiMedia Laboratories, India. Trehalose was purchased from Tokyo Chemical Industry, Japan. Distilled water was filtered by Merck Millipore dual filtration system, India. All other chemicals were of analytical grade and purchased from various vendors.

Methods. *Preparation of PLGA and PLGA−CS Composite NPs.* PLGA NPs were prepared by the double emulsion solvent evaporation method. In brief, PLGA was dissolved into DCM with the ratio of 2.9% w/v, and 200 μL of water was added into the PLGA solution and sonicated for 30 s at an output level of 1 to form the primary emulsion (water-in-oil) (w/o) in ice to avoid high temperature, which damages protein. The primary emulsion was added dropwise into 2.5% PVA solution under homogenization for 15 min at 14,500 rpm on ice to form a secondary (water-in-oil-in-water) emulsion. This emulsion was poured into 2.5% PVA and put on a magnetic starrier to stir overnight at ambient temperature to allow for DCM evaporation. NPs were collected by the centrifugation method after diluting with water at 24,000 rpm for 45 min at 4 °C. The pellet was redispersed into water (Milli-Q) and washed three times to remove all residues of PVA. Trehalose was added as a cryoprotectant and stored overnight at freezing conditions and then lyophilized. The BSA-loaded PLGA NPs were prepared by adding 200 μL BSA (1 mg/mL) solution in place of 200 μL 1× PBS.

Composite NPs were synthesized by functionalization of the carboxylic acid (−COOH) group present on the surface of PLGA NPs by EDC NHS reaction. In brief, 25 mg of PLGA NPs was resuspended into 1 mL dH_2O and added dropwise into 5 mL of 1× PBS buffer (pH 7.4) on a magnetic stirrer. Thereafter, 40 mg of EDC and 20 mg NHS were added into the buffer to react at room temperature for 15 min. Now activated PLGA NPs were added into 20 mL of 0.1% CS solution dropwise and kept overnight for stirring on the magnetic stirrer. NPs were collected by centrifugation at 22,000 rpm at 4 °C for 45 min and washed three times with water to remove excess coupling reagent.

Characterization of CS PLGA Composite NPs. The PLGA NPs and CS PLGA composite NPs were characterized based on size, charge, encapsulation efficiency, PDI, FTIR, surface morphology, the efficacy of protein loading, the integrity of the encapsulated protein, uptake by cells, and in-vitro release of protein as per standard procedure mentioned below.

Size, Zeta Potential, and PDI. The size, zeta potential, and PDI of protein-loaded composite NPs were determined by a dynamic light scattering-based zetasizer (Nano ZS-90, Malvern Instruments, UK). NPs were suspended in water and used for size recording in triplicate. The zeta potential of composite NPs was measured using a specific cuvette by Zetasizer (Malvern Instruments, UK). The zeta potential of PLGA NPs and composite NPs was recorded in a triplicate manner with loaded with BSA and without BSA.

Encapsulation Efficiency. The encapsulation efficiency of BSA loaded into composite NPs was determined by an indirect method. In this study, the BSA amount was estimated into supernatants after collecting NPs by centrifugation. The amount of BSA was calculated by Lowry's method. Encapsulation efficiency was calculated by the following equation:

$$\begin{aligned}\text{EE}\ (\%) = {} & (\text{total amount of therapeutic protein added} \\ & - \text{free therapeutic protein in the supernatant}) \\ & /(\text{total amount of therapeutic protein added}) \\ & \times 100\end{aligned}$$

Protein Loading. The protein loading was estimated in NPs. In brief, 5 mg of BSA composite NPs was dispersed into 100 μL of DCM and vortexed for 30 min, and then 100 μL of PBS buffer (pH = 7.4) was added and vortexed again for 30 min. NPs were centrifuged at 12,000 rpm for 15 min at 4 °C and collected in the middle aqueous part of the tube. The collected part was analyzed for protein estimation by Lowry's method. The percentage of protein loading was calculated using the following formula:

$$\text{protein loading}\ (\%) = \frac{\text{weight of the drug in nanoparticles}}{\text{weight of the nanoparticles}} \times 100$$

Integrity of Encapsulated Protein. The integrity of the encapsulated protein into composite NPs was characterized by running on SDS-PAGE gel electrophoresis and native gel electrophoresis. In brief, in SDS-PAGE electrophoresis, 3 mg of NPs was taken to extract protein as per the method mentioned in the protein loading section. The extracted BSA protein from NPs was loaded on gel, and electrophoresis was performed at a constant current. For native gel electrophoresis,

https://doi.org/10.1021/acsomega.3c00738
ACS Omega 2023, 8, 18751−18759

3 mg of the protein-loaded NPs was dissolved into 100 μL of DCM and vortexed for 30 min and then 100 μL of PBS buffer (pH = 7.4) was added and vortexed again. Subsequently, the mixture was centrifuged to collect the aqueous phase, and this was mixed with 4× loading dye and loaded into the well of native gel. The electrophoresis was performed at a constant current.

Scanning Electron Microscope. The morphology of composite NPs was analyzed by SEM. In brief, lyophilized NPs were mounted on the stub with the help of double-sided adhesive carbon tape. The surface of NPs was made conductive by coating them with a thin layer of gold. The gold-coated samples were examined under a vacuum by a scanning electron microscope (Field emission scanning electron microscope NOVA NANOSEM 450, Thermo Fisher, Netherlands).

Transmission Electron Microscope. The actual size and uniformity of NPs were studied by TEM (FEI-Tecnai G2 12 Twin TEM, Thermo Fisher, Netherlands). The NP sample for TEM analysis was prepared by positioning a drop of sample suspension on a carbon-coated copper grid. The grid was dried in a desiccator under vacuum at room temperature and examined under TEM at an accelerating voltage of 120 kV.

FTIR Analysis. To confirm the composite nature of NPs and encapsulation of BSA into NPs, FT-IR spectra of NPs were obtained. A lyophilized NP was used in this study. In brief, 2 mg of NPs was mixed with the dry potassium bromide (KBr) by grinding. A uniform sheet was made by a tablet press as a background. With air as the background, the wavenumber range was set to 400−4,000 cm^{-1}, and the resolution was set to 2 cm^{-1} recorded by Perkin Elmer Spectrum 2.

X-rays Diffraction Study. XRD analysis was done to analyze the crystallinity of the NPs. XRD patterns were obtained at room temperature using a very high-resolution Cu Kα radiation diffraction system (PAN analytical XRD system) operating at a voltage of 40 kV and current of 30 mA. The XRD pattern of each sample was measured from 10 to 70° 2θ using a step increment of 0.002 2-theta degrees and a scan size of 2°/min.

In Vitro Release Profiles. The release profile of the BSA-loaded nanocomposite was analyzed in a PBS buffer of pH 7.4 over 96 h. 40 mL of PBS buffer was taken into 50 mL of a standing falcon, and 1 mL of NP was taken and kept in an incubator at 37 °C and 80 rpm for incubation. 1 mL of the sample was taken out at the predetermined time, and fixed volume was maintained by adding 1 mL of PBS buffer from outside at each time point and stored at −20 °C for further analysis. The release of protein from NPs was quantified by Lowry's assay. This experiment was performed in triplicate, and the average value with standard deviation was plotted at different time points.

Uptake of Composite NPs. The uptake of composite NPs was studied in cell line A549. In this study, FITC dye-loaded NPs were used. In brief, 1 × 10^5 cells/well were seeded into the 24-well culture plate and incubated to reach up to 70% confluence. Cells were exposed to 100 μg/mL blank NPs, FITC-loaded PLGA NPs, or FITC dye-loaded PLGA−CS composite NPs for 4 h. At the end of the incubation time, extracellular NPs were removed by washing with PBS buffer. Cells were analyzed on a flow cytometer (FACS Calibre, BD Biosciences, USA). During analysis, 10,000 cells were acquired. The FL-1 detector was used to collect the fluorescence of FITC dye. The setting of equipment was done by using the cells incubated with blank NPs. The gating was done for high fluorescence intensity of cells, and blank NP-incubated cells were used as negative control in this experiment.

Cytotoxicity of Composite NPs. Evaluation of the compatibility of composite NPs was performed in in vitro studies. A549 cells were exposed to composite NPs, and cytotoxicity was measured based on a resazurin assay.[34] In brief, 1 × 10^4 cells per well were seeded into a sterile 96-well cell culture plate with DMEM media to reach up to 70% confluency. Cells were exposed with 100 μg/mL of NPs for 24 and 48 h. Resazurin dye was added to each well at the end of incubation time and incubated for 4 h in dark. The cell viability was measured at wavelength (excitation λ 530 nm, emission λ 590 nm) by multimode plate reader (Synergy HTX, BioTek, USA). The results were analyzed as the percentage of reduction in cell growth/viability compared to untreated control wells as a negative control.

Statistical Analysis. The data were recorded in triplicates and expressed as mean ± standard deviation. The value of $p < 0.05$ was regarded as statistically significant and marked as * data presented in the article. Data analysis was performed in MS office excel program by *t*-test analysis (two sample assuming equal variances) with a preferred alpha range of 0.05.

AUTHOR INFORMATION

Corresponding Authors

Mohd. Sohail Akhtar − *Molecular and Structural Biology Division, CSIR-Central Drug Research Institute, Lucknow 226031, India*; Email: sohail@cdri.res.in

Awadh Bihari Yadav − *Centre of Biotechnology, University of Allahabad, Prayagraj 211002, India*; orcid.org/0000-0003-2801-5071; Email: awadhyadav@allduniv.ac.in

Authors

Manish Gaur − *Centre of Biotechnology, University of Allahabad, Prayagraj 211002, India*

Sarita Maurya − *Centre of Biotechnology, University of Allahabad, Prayagraj 211002, India*

Complete contact information is available at: https://pubs.acs.org/10.1021/acsomega.3c00738

Notes

The authors declare no competing financial interest.

ACKNOWLEDGMENTS

M.G. and S.M. acknowledged UGC and CSIR for Ph.D. scholarship and Senior research fellowship. IIT Kanpur U.P., India for providing SEM, TEM, XRD, facility, and CSIR-CDRI SAIF for flow cytometry analysis. This project is funded under core grant no. CRG/0021135/2019 of Science and Engineering Research Board (SERB), Department of Science and Technology, Govt. India.

REFERENCES

(1) Patra, J. K.; Das, G.; Fraceto, L. F.; Campos, E. V. R.; Rodriguez-Torres, M. d. P.; Acosta-Torres, L. S.; Diaz-Torres, L. A.; Grillo, R.; Swamy, M. K.; Sharma, S.; et al. Nano based drug delivery systems: recent developments and future prospects. *J. Nanobiotechnol.* **2018**, *16*, 71.

(2) Elmowafy, E. M.; Tiboni, M.; Soliman, M. E. Biocompatibility, biodegradation and biomedical applications of poly(lactic acid)/poly(lactic-co-glycolic acid) micro and nanoparticles. *J. Pharm. Invest.* **2019**, *49*, 347−380.

https://doi.org/10.1021/acsomega.3c00738
ACS Omega 2023, 8, 18751−18759

(3) Jennings, J. A.; Wells, C. M.; McGraw, G. S.; Velasquez Pulgarin, D. A.; Whitaker, M. D.; Pruitt, R. L.; Bumgardner, J. D. Chitosan coatings to control release and target tissues for therapeutic delivery. *Ther. Deliv.* **2015**, *6*, 855−871.
(4) Ali, A.; Ahmed, S. A review on chitosan and its nanocomposites in drug delivery. *Int. J. Biol. Macromol.* **2018**, *109*, 273−286.
(5) Salatin, S.; Maleki Dizaj, S.; Yari Khosroushahi, A. Effect of the surface modification, size, and shape on cellular uptake of nanoparticles. *Cell Biol. Int.* **2015**, *39*, 881−890.
(6) Devulapally, R.; Paulmurugan, R. Polymer nanoparticles for drug and small silencing RNA delivery to treat cancers of different phenotypes. *Wiley Interdiscip. Rev.: Nanomed. Nanobiotechnol.* **2014**, *6*, 40−60.
(7) Hajavi, J.; Ebrahimian, M.; Sankian, M.; Khakzad, M. R.; Hashemi, M. Optimization of PLGA formulation containing protein or peptide-based antigen: Recent advances. *J. Biomed. Mater. Res., Part A* **2018**, *106*, 2540−2551.
(8) De Negri Atanasio, G.; Ferrari, P. F.; Campardelli, R.; Perego, P.; Palombo, D. Poly (Lactic-co-Glycolic Acid) Nanoparticles and Nanoliposomes for Protein Delivery in Targeted Therapy: A Comparative In Vitro Study. *Polymer* **2020**, *12*, 2566.
(9) Elbatanony, R. S.; Parvathaneni, V.; Kulkarni, N. S.; Shukla, S. K.; Chauhan, G.; Kunda, N. K.; Gupta, V. Afatinib-loaded Inhalable PLGA Nanoparticles for Localized Therapy of Non-Small Cell Lung Cancer (NSCLC) − Development and In-vitro Efficacy. *Drug Delivery Transl. Res.* **2021**, *11*, 927−943.
(10) Ha, H. K.; Kim, J. W.; Lee, M. R.; Jun, W.; Lee, W. J. Cellular uptake and cytotoxicity of β-lactoglobulin nanoparticles: The effects of particle size and surface charge. *Asian-Australas. J. Anim. Sci.* **2015**, *28*, 420−427.
(11) Muralidharan, P.; Malapit, M.; Mallory, E.; Hayes, D.; Mansour, H. M. Inhalable nanoparticulate powders for respiratory delivery. *Nanomed. Nanotechnol. Biol. Med.* **2015**, *11*, 1189−1199.
(12) Yu, Z.; Yu, M.; Zhang, Z.; Hong, G.; Xiong, Q. Bovine serum albumin nanoparticles as controlled release carrier for local drug delivery to the inner ear. *Nanoscale Res. Lett.* **2014**, *9*, 343−347.
(13) Ma, F. K.; Li, J.; Kong, M.; Liu, Y.; An, Y.; Chen, X. G. Preparation and hydrolytic erosion of differently structured PLGA nanoparticles with chitosan modification. *Int. J. Biol. Macromol.* **2013**, *54*, 174−179.
(14) Wang, Y.; Li, P.; Kong, L. Chitosan-modified PLGA nanoparticles with versatile surface for improved drug delivery. *AAPS PharmSciTech* **2013**, *14*, 585−592.
(15) Danaei, M.; Dehghankhold, M.; Ataei, S.; Hasanzadeh Davarani, F.; Javanmard, R.; Dokhani, A.; Khorasani, S.; Mozafari, M. Impact of Particle Size and Polydispersity Index on the Clinical Applications of Lipidic Nanocarrier Systems. *Pharmaceutics* **2018**, *10*, 57.
(16) Badran, M. FORMULATION AND IN VITRO EVALUATION OF FLUFENAMIC ACID LOADED DEFORMABLE LIPOSOMES FOR IMPROVED SKIN DELIVERY. *Dig. J. Nanomater. Biostruct.* **2014**, *9*, 83−91.
(17) Cruz, K. P.; Patricio, B. F. C.; Pires, V. C.; Amorim, M. F.; Pinho, A. G. S. F.; Quadros, H. C.; Dantas, D. A. S.; Chaves, M. H. C.; Formiga, F. R.; Rocha, H. V. A.; et al. Development and Characterization of PLGA Nanoparticles Containing 17-DMAG, an Hsp90 Inhibitor. *Front. Chem.* **2021**, *9*, 295.
(18) McCall, R. L.; Sirianni, R. W. PLGA Nanoparticles Formed by Single- or Double-emulsion with Vitamin E-TPGS. *JoVE* **2013**, *82*, No. e51015.
(19) Azizi, M.; Farahmandghavi, F.; Joghataei, M.; Zandi, M.; Imani, M.; Bakhtiary, M.; Dorkoosh, F. A.; Ghazizadeh, F. Fabrication of protein-loaded PLGA nanoparticles: Effect of selected formulation variables on particle size and release profile. *J. Polym. Res.* **2013**, *20*, 110−114.
(20) Kang, B. S.; Choi, J. S.; Lee, S. E.; Lee, J. K.; Kim, T. H.; Jang, W. S.; Tunsirikongkon, A.; Kim, J. K.; Park, J. S. Enhancing the in vitro anticancer activity of albendazole incorporated into chitosan-coated PLGA nanoparticles. *Carbohydr. Polym.* **2017**, *159*, 39−47.
(21) Arafa, M. G.; Mousa, H. A.; Afifi, N. N. Preparation of PLGA-chitosan based nanocarriers for enhancing antibacterial effect of ciprofloxacin in root canal infection. *Drug Deliv.* **2019**, *27*, 26−39.
(22) Kashyap, S.; Singh, V.; Singh, A.; Mishra, A. Enhanced sustained release of furosemide in long circulating chitosan-conjugated PLGA nanoparticles. *Res. Pharm. Sci.* **2019**, *14*, 93.
(23) Yadav, A. K.; Mishra, P.; Mishra, A. K.; Mishra, P.; Jain, S.; Agrawal, G. P. Development and characterization of hyaluronic acid−anchored PLGA nanoparticulate carriers of doxorubicin. *Nanomed. Nanotechnol. Biol. Med.* **2007**, *3*, 246−257.
(24) Guo, M.; Rong, W. T.; Hou, J.; Wang, D. F.; Lu, Y.; Wang, Y.; Yu, S. Q.; Xu, Q. Mechanisms of chitosan-coated poly(lactic-co-glycolic acid) nanoparticles for improving oral absorption of 7-ethyl-10-hydroxycamptothecin. *Nanotechnology* **2013**, *24*, 245101.
(25) Park, M. H.; Baek, J. S.; Lee, C. A.; Kim, D. C.; Cho, C. W. The effect of Eudragit type on BSA-loaded PLGA nanoparticles. *J. Pharm. Invest.* **2014**, *44*, 339−349.
(26) Vaidya, B.; Kulkarni, N. S.; Shukla, S. K.; Parvathaneni, V.; Chauhan, G.; Damon, J. K.; Sarode, A.; Garcia, J. V.; Kunda, N.; Mitragotri, S.; et al. Development of inhalable quinacrine loaded bovine serum albumin modified cationic nanoparticles: Repurposing quinacrine for lung cancer therapeutics. *Int. J. Pharm.* **2020**, *577*, 118995.
(27) Jin, M.; Seo, S. H.; Kim, B. S.; Hwang, S.; Kang, Y. G.; Shin, J. W.; Cho, K. H.; Byeon, J.; Shin, M. C.; Kim, D.; et al. Combined Application of Prototype Ultrasound and BSA-Loaded PLGA Particles for Protein Delivery. *Pharm. Res.* **2021**, *38*, 1455−1466.
(28) Erdoğar, N.; Akkın, S.; Nielsen, T. T.; Özçelebi, E.; Erdoğdu, B.; Nemutlu, E.; İskit, A. B.; Bilensoy, E. Development of oral aprepitant-loaded chitosan−polyethylene glycol-coated cyclodextrin nanocapsules: formulation, characterization, and pharmacokinetic evaluation. *J. Pharm. Invest.* **2021**, *51*, 297−310.
(29) Zeb, A.; Gul, M.; Nguyen, T. T. L.; Maeng, H. J. Controlled release and targeted drug delivery with poly(lactic-co-glycolic acid) nanoparticles: reviewing two decades of research. *J. Pharm. Invest.* **2022**, *52*, 683−724.
(30) Wiggins, J. S.; Hassan, M. K.; Mauritz, K. A.; Storey, R. F. Hydrolytic degradation of poly(d,l-lactide) as a function of end group: Carboxylic acid vs. hydroxyl. *Polymer* **2006**, *47*, 1960−1969.
(31) Nag, S.; Das Saha, K. Chitosan-Decorated PLGA-NPs Loaded with Tannic Acid/Vitamin e Mitigate Colon Cancer via the NF-κB/β-Cat/EMT Pathway. *ACS Omega* **2021**, *6*, 28752−28769.
(32) Tahara, K.; Sakai, T.; Yamamoto, H.; Takeuchi, H.; Hirashima, N.; Kawashima, Y. Improved cellular uptake of chitosan-modified PLGA nanospheres by A549 cells. *Int. J. Pharm.* **2009**, *382*, 198−204.
(33) Van Hees, S.; Elbrink, K.; De Schryver, M.; Delputte, P. L.; Kiekens, F. Improving cellular uptake and cytotoxicity of chitosan-coated poly(lactic-co-glycolic acid) nanoparticles in macrophages. *Nanomedicine* **2020**, *15*, 2671−2688.
(34) Agarwal, S.; Mohamed, M. S.; Mizuki, T.; Maekawa, T.; Sakthi Kumar, D. Chlorotoxin modified morusin−PLGA nanoparticles for targeted glioblastoma therapy. *J. Mater. Chem. B* **2019**, *7*, 5896−5919.

https://doi.org/10.1021/acsomega.3c00738
ACS Omega 2023, 8, 18751−18759